(10) Solomon, I. *Phys. Rev.* **1955**, *94*, 559.
(11) Jones, G. P. *Phys. Rev.* **1966**, *148*, 332.
(12) Bloembergen, N.; Purcell, E. M.; Pound, R. V. *Phys. Rev.* **1948**, *73*, 679.
(13) Woessner, D. E.; *J. Chem. Phys.* **1962**, *30*, 1.
(14) McCall, D. W.; Douglas, D. C.; Anderson, E. W. *J. Chem. Phys.* **1959**, *30*, 1272.
(15) Heatley, F.; Began, A. *Polymer* **1970**, *17*, 399.
(16) Schaefer, J. *Macromolecules* **1973**, *6*, 882.
(17) Ghesquiere, D.; Ban, B.; Chachaty, C. *Macromolecules* **1977**, *10*, 743.
(18) Glarum, S. H. *J. Chem. Phys.* **1960**, *33*, 639.
(19) Hunt, B. I.; Powles, J. G. *Proc. Phys. Soc.* **1966**, *88*, 513.
(20) Valeur, B.; Jarry, J. P.; Geny, F.; Monnerie, L. *J. Polym. Sci., Polym. Phys. Ed.* **1975**, *13*, 667.
(21) Valeur, B.; Monnerie, L.; Jarry, J. P. *J. Polym. Sci., Polym. Phys. Ed.* **1975**, *13*, 675.
(22) Valeur, B.; Jarry, J. P.; Geny, F.; Monnerie, L. *J. Polym. Sci., Polym. Phys. Ed.* **1975**, *13*, 2251.
(23) Gronski, W.; Murayama, N. *Makromol. Chem.* **1978**, *179*, 1521.
(24) Gronski, W. *Makromol. Chem.* **1979**, *180*, 1119.
(25) Gutowsky, H. S.; Pake, G. E. *J. Chem. Phys.* **1950**, *18*, 162.
(26) Williams, G.; Watts, D. C. *Trans. Faraday Soc.* **1970**, *66*, 80.
(27) For a history of the fractional exponential function going back to Kohlrausch (1866) see: Struik, L. C. E. Abstracts of 10th Europhysics Conference on Macromolecular Physics, 1980, p 135.
(28) Ngai, K. L. *Comments Solid State Phys.* **1979**, *9*, 127–147.
(29) Ngai, K. L.; White, C. T. *Phys. Rev. B* **1979**, *20*, 2475.
(30) Ngai, K. L. *Phys. Rev. B* **1980**, *22*, 2066.
(31) McCrum, N. G.; Read, B. E.; Williams, G. "Anelastic and Dielectric Effects in Polymeric Solids"; Wiley: London, 1967.
(32) See: DeVault, G. P.; McClennan, J. A. *Phys. Rev.* **1965**, *137*, A724. Zwanzig, R. *J. Chem. Phys.* **1965**, *43*, 714.
(33) Bendler, J. T. *Ann. N.Y. Acad. Sci.* **1981**, *371*, 299.
(34) Tonelli, A. E. *Macromolecules* **1972**, *5*, 558.
(35) Dewar, M. J.; Thiele, W. *J. Am. Chem. Soc.* **1977**, *99*, 4899.
(36) O'Gara, J. F.; Desjardins, S. G.; Jones, A. A. *Macromolecules* **1981**, *14*, 64.
(37) Erman, B.; Marvin, D. C.; Flory, P. J. *Bull. Am. Phys. Soc.* **1981**, *26*, 227.
(38) Binkley, J. S.; Whiteside, R. A.; Kirshnan, R.; Seeger, R.; DeFrees, D. J.; Schlegel, H. B.; Topoil, S.; Kahn, L. R.; Pople, J. A. *QCPE* **1980**, *No. 406*.
(39) Spiess, H. W. International Union of Pure and Applied Chemistry, 28th Macromolecular Symposium Proceedings, 1982, p 35.
(40) Schaefer, J.; Sefcik, M. D.; Stejskal, E. O.; McKay, R. A.; Dixon, W. T., ref 39, p 25.
(41) Garroway, A. N.; Ritchey, W. M.; Moniz, W. B., ref 39, p 1.

Thermal and Mechanical Properties of a Poly(ethylene oxide-*b*-isoprene-*b*-ethylene oxide) Block Polymer Complexed with NaSCN

C. Robitaille and J. Prud'homme*

Department of Chemistry, University of Montreal, Montreal, Quebec, Canada H3C 3V1.
Received August 30, 1982

ABSTRACT: The changes in thermal and mechanical properties produced by complexation with NaSCN of a poly(ethylene oxide-*b*-isoprene-*b*-ethylene oxide) (PEO–PI–PEO) block polymer are described. The number-average molecular weight of the PEO–PI–PEO polymer was 1.67×10^5, and its PEO weight fraction was 0.14. It is shown that complexation, which occurs selectively with the PEO end blocks, can yield a semicrystalline thermoplastic elastomer that melts at about 450 K. The main characteristics of the complexed block polymer are a crystallization temperature, which occurs 90 K lower than that of complexed homo-PEO, and good dimensional stability at high temperature. However, the tensile strength of the complexed material appears to be considerably reduced with increasing temperature. A pronounced supercooling was also observed for the uncomplexed PEO–PI–PEO block polymer. This phenomenon seems to be a general feature of two-phase block polymers in which the crystallizable component is finely dispersed into isolated microdomains.

Introduction

Elastomeric ABA block polymers with crystalline end blocks have received increasing interest during the last decade.[1–7] Most investigations dealing with this class of block polymers have been oriented toward the development of novel thermoplastic elastomers possessing mechanical properties that compare favorably with those of the more conventional completely amorphous ABA block polymers, such as styrene–diene three-block polymers, but having a better dimensional stability at high temperature and/or a better resistance to solvents. Typical examples of such materials are those based on poly(ethylene sulfide),[1] polypivalolactone,[4] and hydrogenated 1,4-polybutadiene[5,6] end blocks. Also reported in the literature are data concerning ABA materials based on polythiacyclobutane[2] (PTCB) and poly(ethylene oxide)[3] (PEO) end blocks. Though the melting temperatures of PTCB and PEO are not high enough for considering elastomeric applications of the block polymers, these latter materials, which dissolved in aromatic solvents at moderate temperature, were good model systems for studying the role of the casting solvent and temperature on the morphology of the crystalline microdomains in specimens prepared by solvent casting.[2,3] In both cases it was shown that well-defined spherical or cylindrical crystalline microdomains were formed when the casting solvent and temperature were such that liquid–liquid phase separation occurred before crystallization.[2,3]

In the present paper, we describe the changes in physical and mechanical properties produced when a poly(ethylene oxide-*b*-isoprene-*b*-ethylene oxide) (PEO–PI–PEO) block polymer having a number-average molecular weight of 1.67×10^5 and a PEO weight fraction of 0.14 is complexed with NaSCN. It is known that PEO forms crystalline ionic complexes with a range of compounds including alkali metal and ammonium salts.[8–10] Wright[8] reported that ammonium, potassium, and sodium thiocyanate form crystalline complexes with PEO whose melting temperatures increase with decreasing cation size (T_m = 343, 373, and 468 K for NH_4^+, K^+, and Na^+, respectively). The admitted stoichiometry for these complexes is 4 mol of PEO monomer unit for 1 mol of cation.[8,10] The high melting temperature of the PEO·NaSCN complex together with its observed stability upon melt recrystallization were the major reasons for investigating the present system. The materials were studied under the form of films pre-

0024-9297/83/2216-0665$01.50/0 © 1983 American Chemical Society

Table I
Molecular Characteristics of the Materials Studied in the Present Work

sample	$M_n \times 10^{-3}$	PEO weight fraction	PI microstructure,[c] mol fraction 1,4(cis-trans)	1,2	3,4
PEO-PI-PEO	167[a]	0.14[c]	0.15	0.35	0.50
PI-95K	95[a]		0.15	0.35	0.50
PEO-4K	3.9[b]				

[a] Measured by membrane osmometry. [b] Measured by vapor pressure osmometry. [c] Determined from ^{1}H NMR spectra measured at 220 MHz.

pared by solvent casting. The changes in thermal properties produced by complexation were investigated by differential scanning calorimetry (DSC). Also studied by DSC was the melt crystallization behavior of both the uncomplexed and complexed materials. The changes in mechanical properties produced by either complexation of melt recrystallization were investigated by stress–strain measurements.

Experimental Section

Materials. The PEO–PI–PEO block polymer was prepared by anionic polymerization with potassium naphthalene as initiator and tetrahydrofuran (THF) as solvent. The polymerization was carried out in an evacuated and sealed all-glass reaction vessel by using the break-seal technique. In a first step, the isoprene monomer was polymerized at 233 K for a period of 6 h. In a second step, the ethylene oxide monomer was added to the difunctional poly(isoprenylpotassium) solution and the temperature was increased to 298 K. Then the reaction was allowed to proceed for an additional period of 72 h. At the end of this period, the reaction was terminated by adding a dilute solution of glacial acetic acid in THF. The block polymer was isolated by precipitation at 283 K in anhydrous ethanol containing 0.03% of the antioxidant 2,6-di-*tert*-butyl-*p*-cresol. The precipitate was dried to constant weight under high vacuum and stored under vacuum. Also used in the present work was a polyisoprene sample prepared under the same conditions as the PI block in the block polymer and a low-molecular-weight PEO sample obtained from Dow Chemical Co. The molecular characteristics of the three samples are given in Table I. Figure I shows the GPC traces of the three samples together with that of a Waters polystyrene standard of low polydispersity. The GPC measurements were recorded by using a Waters Associates Model 200 instrument with a series arrangement of four Waters Styragel columns with upper porosity designations of 10^6, 10^5, 10^4, and 10^3 Å. The solvent was reagent grade THF containing 0.03% of the already mentioned antioxidant and the temperature was 308 K. Flow rate was 1 mL/min, and a 2-mL portion of solution, 2.5×10^{-3} g/mL concentration, was injected in each case. Comparison of the GPC traces in Figure 1 shows unimodal curves for all the samples with a slightly broader peak for the block polymer sample. The microstructure of the PI block in the block polymer, as well as that of the PI sample, was determined from ^{1}H NMR spectra measured at 220 MHz, according to the assignations reported by Pham and Petiaud.[11] The results are reported in Table I.

Specimen Preparations. The PEO–PI–PEO block polymer was complexed with NaSCN by adding a methanol solution of anhydrous NaSCN to a 1% benzene solution of the block polymer. The mixture contained 4 mol of PEO monomer unit for 1 mol of NaSCN. Its methanol volume fraction was 0.17. Under these conditions, a homogeneous clear solution was obtained from which transparent film specimens about 0.5 mm thick were prepared by solvent evaporation on a mercury surface. The solvents were slowly evaporated at room temperature over a period of 10 days in a chamber flushed by dry nitrogen. The film specimens were subsequently dried for a week under high vacuum and stored under vacuum. The PEO homopolymer sample was complexed with NaSCN by adding a 5% methanol solution of NaSCN to a 5% methanol solution of the PEO sample. The PEO·NaSCN complex, which contained 4 mol of PEO monomer unit for 1 mol

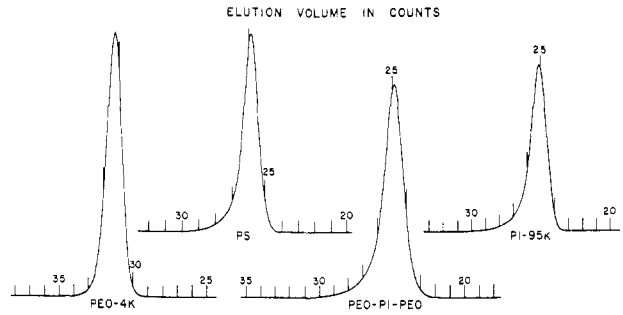

Figure 1. GPC elution curves for the PEO–PI–PEO block polymer sample, PEO-4K poly(ethylene oxide) sample, PI-95K polyisoprene sample, and polystyrene standard ($M_n = 1.10 \times 10^5$, $M_w/M_n = 1.02$).

of NaSCN, was isolated by solvent evaporation and dried under high vacuum. Prior to the complexation, the PEO sample was purified by precipitation in petroleum ether from a 5% THF solution followed by drying at 343 K under high vacuum. Film specimens of both the uncomplexed PEO–PI–PEO block polymer and the PI sample were prepared by solvent casting from 4% benzene solutions. The solvent was slowly evaporated on a mercury surface and the film specimens, about 0.5 mm thick, were dried under high vacuum for a week and stored under vacuum. All the solvents used for the above specimen preparations were reagent grade materials carefully dried before utilization. The specimens containing NaSCN were handled under dry atmosphere.

DSC Measurements. Glass transition, melting, and crystallization curves were recorded with a Perkin-Elmer Model DSC-IB differential scanning calorimeter. Sample sizes were in the range 17–22 mg. Heating and cooling rates were 10 K/min and 5 K/min, respectively. Heating curves of the as cast block polymer specimens were measured after cooling from room temperature to 220 K. Calibration of the temperature scale was made with standard materials of melting points in the range 234–505 K. Heat of fusion of poly(ethylene oxide) was calculated by comparison with the peak area measured on the melting curve of azobenzene ($T_m = 341$ K, $\Delta H_f = 121.0$ J/g). Degree of crystallinity of poly(ethylene oxide) was estimated from the ratio of the experimentally determined heat of fusion and the value of 203 ± 3 J/g reported in the literature for the heat of fusion of 100% crystalline PEO.[12]

Stress–Strain Measurements. Stress–strain curves were measured with an Instron Model 1130 tensile tester. An environmental chamber was used to obtain data at constant temperature. Test specimens were 20 mm in length and 2 mm in width. Crosshead speed was 4 mm/min.

Small-Angle X-ray Scattering Measurements. Small-angle X-ray scattering photographs were taken with a Model 2202 Rigaku-Denki goniometer provided with a two-pinhole collimator. Ni-filtered Cu Kα radiation ($\lambda = 0.154$ nm) was generated by a Philips tube operated at 40 kV and 20 mA. The second pinhole, specimen, and photographic film were placed at 300, 320, and 630 mm from the first pinhole, respectively. The diameters of the first and second pinholes were 0.3 and 0.2 mm, respectively. The radial profile of the scattering intensity was recorded from the photographic films by means of Joyce-Loebl microdensitometer.

Heat Treatment of the Film Specimens. Heat treatment of the complexed and uncomplexed PEO–PI–PEO film specimens was carried out with an environmental chamber flushed with temperature-controlled dry nitrogen. The specimens cut into rectangular strips 20 mm long and 5 mm wide were held into a rectangular Teflon frame of about the same size lying on a Teflon plate. The temperature was monitored by means of a thermocouple lying close to the specimen. Cooling rate was bout 5 K/min. No significant change in film thickness was observed when measured after heat treatment.

Results and Discussion

(a) Thermal Properties of the Starting Material. Figure 2 shows the DSC heating curve measured at 10

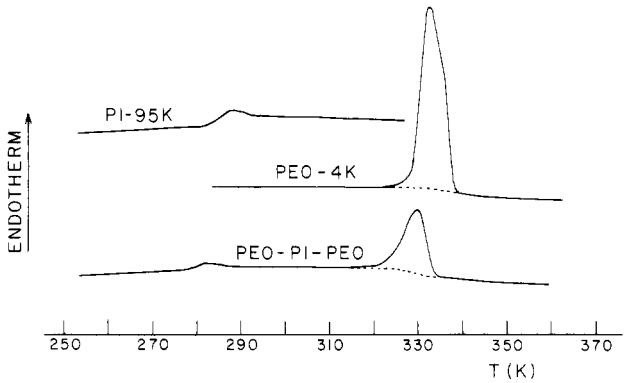

Figure 2. DSC heating curves measured at 10 K/min for the PEO–PI–PEO block polymer sample as cast from benzene solution, PEO-4K poly(ethylene oxide) sample, and PI-95K polyisoprene sample. Both the PEO–PI–PEO and the PI-95K samples were cooled from room temperature to 220 K at 5 K/min before measurement.

K/min on the three-block polymer sampled PEO–PI–PEO cast from benzene solution. Also shown in Figure 2 are the DSC curves measured on the polyisoprene sample PI-95K and the poly(ethylene oxide) sample PEO-4K. From Figure 2 it may be seen that the block polymer sample exhibits a glass transition at a temperature close to that of the homo-PI sample together with a melting peak that is also in the vicinity of that of the homo-PEO sample. Quantitative analysis of the melting peaks in Figure 2 indicated degrees of crystallinity of 69% and 96% for the PEO moiety in the block polymer and the homo-PEO, respectively. Also evident in Figure 2 is a melting point depression for the block polymer. Such a behavior, i.e., lower melting point and lower crystallinity of the PEO microdomains when compared to homo-PEO, seems to be a general characteristic of block polymers having a minor amount of PEO. It has already been observed not only for PEO–PI–PEO and PEO–PI block polymers having a PI microstructure similar to that in the present material[3] but also for other systems including PEO–PS–PEO, and PS–PEO (PS = polystyrene),[13] and PEMA–PEO (PEMA = poly(ethyl methacrylate)).[14] Both the melting point depression and the lower crystallinity of the PEO microphase in these block polymers have been attributed to the formation of less perfect crystalline lamellae, due to the high dispersion of the PEO component in the amorphous phase.[13,14]

Another characteristic of block polymers having a minor amount of PEO is a PEO crystallization behavior that exhibits considerable supercooling when compared to homo-PEO. This is illustrated in Figure 3, which shows the DSC cooling curves measured at 5 K/min on samples PEO–PI–PEO and PEO–4K, respectively, after melting at 360 K for a period of 15 min. From Figure 3 one can see that the PEO sample crystallizes readily in the vicinity of 315 K while the block polymer sample must be cooled to about 254 K before crystallization can occur. This supercooling is such that even after 1 month of storage at room temperature, a previously melted specimen did not exhibit any melting endotherm upon subsequent heating. In fact, such a pronounced supercooling effect, as well as the existence of two distinct stages for PEO crystallization, has been reported previously for PS–PEO[15,16] and PEO–PS–PEO[16] block polymers. Lotz and Kovacs[15] reported dilatometric measurements made on a PS–PEO sample having a PEO weight fraction close to 0.30, which revealed two distinct crystallization steps at temperatures near 308 and 253 K, respectively. They interpreted this behavior as the result of the segregation of the heterogeneous nuclei

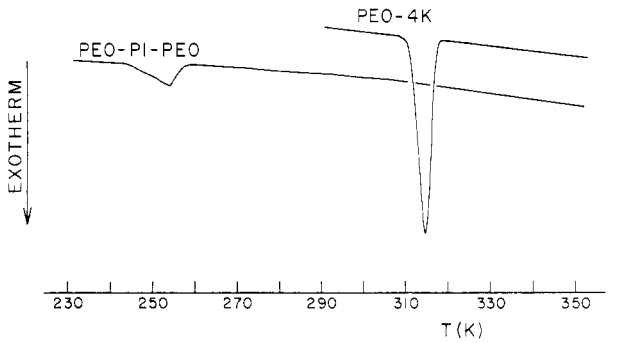

Figure 3. DSC cooling curves measured at 5 K/min for the PEO–PI–PEO block polymer sample and PEO-4K poly(ethylene oxide) sample after melting at 360 K for 15 min.

able to produce crystallization at 308 K into only a fraction of the PEO microdomains present in the system, leaving the PEO microdomains that do not contain heterogeneity free to nucleate at the lower temperature by a homogeneous mechanism. This interpretation pursued the ideas developed by Turnbull[17] for the so-called "droplet experiment", which is a very convenient technique for studying homogeneous nucleation in crystallizable materials including polymers.[18,19] In the droplet experiment, the material under study is finely dispersed in an inert medium in such a way that the heterogeneous nuclei initially present in the material are segregated in a few isolated droplets and thereby cannot contribute to the nucleation of the greater part of the dispersed system.

Recently, O'Malley[16] reported DSC cooling curves measured at 10/K on styrene–ethylene oxide block polymers of various numbers of blocks that all showed two distinct crystallization exotherms near 313 and 253 K, respectively. Among the samples studied by O'Malley there was a PS–PEO sample identical with that studied by Lotz and Kovacs[15] and also a PEO–PS–PEO sample having a PEO weight fraction of 0.30. In both these samples the number-average molecular weight of the PEO blocks was close to 1×10^4, a characteristic that led to a PS block about twice as large in the three-block polymer than in the two-block polymer. As observed on the DSC curves, the crystallization exotherm near 253 K was more important in the case of the three-block polymer, indicating a better dispersion of the PEO phase in that latter case. Therefore, the occurrence of only the low-temperature exotherm in the DSC cooling curve of the present PEO–PI–PEO polymer, as shown on Figure 3, indicates that the PEO melted phase of this polymer is finely dispersed into well-isolated microdomains. Interestingly, despite the differences in both the chemical nature and glass transition temperatures, T_g, of the amorphous blocks in the PEO–PS–PEO and PEO–PI–PEO polymers, both materials exhibit supercooling with crystallization near 254 K when cooled at either 5 or 10 K/min. Thus, the pronounced supercooling phenomenon observed with that type of block polymer is an intrinsic feature of the PEO microphase, a fact that reinforces the interpretation given by Lotz and Kovacs,[15] who attributed this behavior to a homogeneous nucleation process in PEO microdomains free from heterogeneous nuclei.

(b) Thermal Properties of the NaSCN-Complexed Material. Figure 4 shows the DSC heating curve measured at 10 K/min on the as cast PEO–PI–PEO block polymer complexed with NaSCN. Also shown in Figure 4 is the DSC curve measured on sample PEO-4K complexed with the same salt. In both cases, the molar ratio of PEO monomer units to NaSCN was 4. The effect of complexation is readily seen in Figure 4 by the appearance

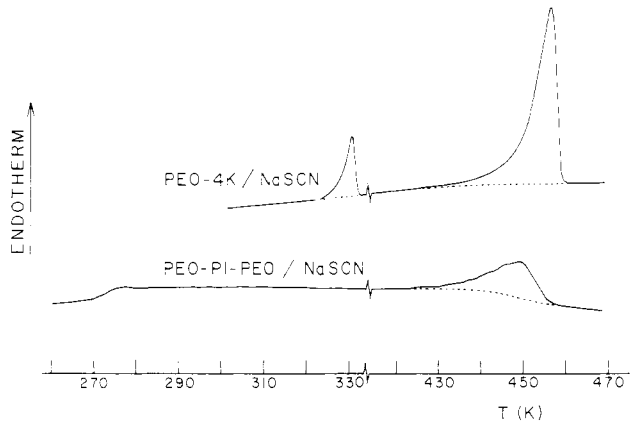

Figure 4. DSC heating curves measured at 10 K/min for the as cast PEO–PI–PEO block polymer and the PEO-4K sample complexed with NaSCN.

of a sharp melting endotherm at 456 K in the case of the complexed PEO-4K sample. Similarly, a high-temperature endotherm is observed at 450 K for the complexed PEO–PI–PEO sample. Inspection of the DSC curve of the PEO-4K sample complexed with NaSCN shows the presence of a second but smaller endotherm at 331 K. The latter appears at a temperature that is only 2 K lower than the melting endotherm observed for the uncomplexed PEO-4K sample. This indicates that the molar ratio of the PEO monomer units to NaSCN of 4 chosen for the present study does not correspond to the exact stoichiometry of the PEO·NaSCN complex. This was confirmed by wide-angle X-ray diffraction measurements, which showed the PEO reflexions in addition to those of the complexed new crystalline entity. The DSC curve of the complexed PEO–PI–PEO sample in Figure 4 does not show any endotherm at 331 K. This may be explained by considering that, as for the uncomplexed PEO–PI–PEO sample, less perfect crystallites are formed in the complexed block polymer due to the high dispersion of the crystallizable microphase. In fact, this effect not only inhibits crystallization of the residual uncomplexed PEO component but also reduces the degree of crystallinity of the complexed component. Although the heat of fusion of 100% crystalline PEO·NaSCN complex is unknown, direct comparison of the heats of fusion per gram of initial PEO estimated from the high-temperature endotherms in curves of Figure 4 indicates that the crystallinity of the complexed PEO moiety in the block polymer is only 37% that of the complexed homo-PEO sample.

Crystallization curves measured at 5 K/min for both the complexed PEO-4K and PEO–PI–PEO materials are shown in Figure 5. The samples were melted at 470 K for 15 min before cooling. From Figure 5, one can see that the complexed PEO sample exhibits two distinct crystallization exotherms at 424 and 303 K, respectively. The former exotherm, which is the most important, is attributed to crystallization of the complexed component while the second exotherm at 303 K, though 12 K lower than that observed in Figure 3 for the homo-PEO sample, corresponds to either crystallization of the residual uncomplexed PEO component under the form of considerably less perfect crystallites than those obtained for homo-PEO or to crystallization of a eutectic mixture of complexed and residual uncomplexed PEO components. As shown in Figure 5, the crystallization curve measured on the complexed PEO–PI–PEO material exhibits a single exotherm at 335 K, which is 89 K lower than the main exotherm observed on the crystallization curve of the complexed homo-PEO sample. Thus, as for the uncomplexed block

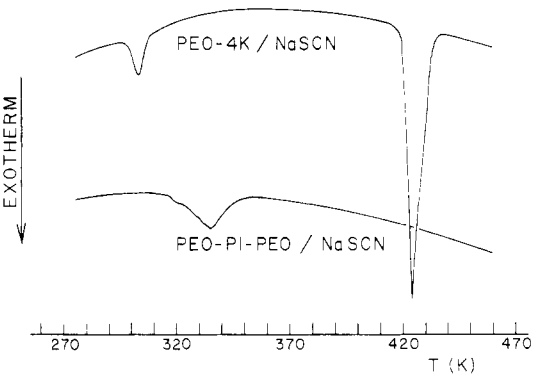

Figure 5. DSC cooling curves measured at 5 K/min for the PEO–PI–PEO block polymer and the PEO-4K sample complexed with NaSCN.

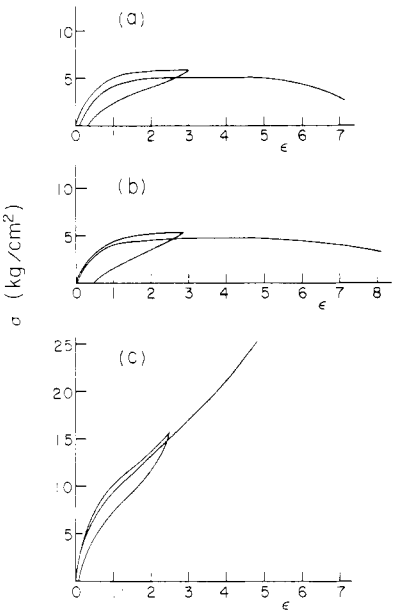

Figure 6. Stress–strain curves measured at 298 K for the PEO–PI–PEO block polymer sample as cast from benzene solution (a), PI-95K polyisoprene un-cross-linked sample (b), and PEO–PI–PEO sample crystallized by slow cooling to 230 K after heating for 15 min at 360 K (c).

polymer, the crystallization behavior of the complexed block polymer is characterized by a substantial supercooling effect due to the high dispersion of the complexed PEO component in the PI rubbery matrix.

(c) Mechanical Properties of the Starting Material. Figure 6a shows stress–strain curves measured at 298 K on the as cast PEO–PI–PEO specimen prepared from benzene solution. Also shown in Figure 6 are stress–strain curves measured at the same temperature on the polyisoprene PI-95K sample (Figure 6b) and on the PEO–PI–PEO specimen crystallized by slow cooling to 230 K after heating for 15 min at 360 K (Figure 6c). In each case is shown a first extension cycle to a strain, ϵ, in the range 2.5–3, followed by a second extension recorded up to rupture. The three specimens were relaxed for 15 min between the first and the second extension. Comparison of Figures 6a and 6c reveals a considerable difference between the mechanical behavior of the as cast specimen and that of the specimen crystallized by cooling to 230 K. The as cast material (Figure 6a) behaves more like the uncross-linked homo-PI sample (Figure 6b). It exhibits necking and rubbery flow at strain $\epsilon > 4$ as inicated by a drop in nominal tensile stress. In contrast, the material crystallized by cooling to 230 K (Figure 6c) exhibits a

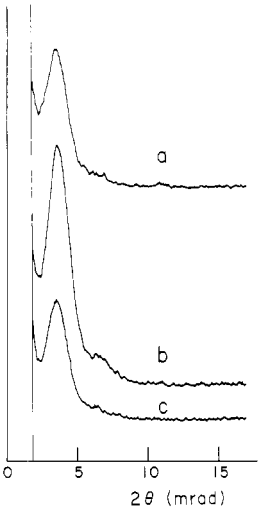

Figure 7. Small-angle X-ray scattering curves measured on the PEO–PI–PEO block polymer sample: (a) as cast from benzene solution, (b) crystallized by slow cooling from 360 to 230 K, (c) supercooled after melting at 360 K and slow cooling to room temperature.

behavior which is characteristic of a thermoplastic elastomer that is a nearly reversible extension cycle together with an increasing stress with increasing strain up to the rupture. The explanation for this difference of behavior is straightforward. In fact, as will be shown in the next paragraph, small-angle X-ray scattering measurements clearly indicate the presence of a nearly identical microphase structure in both the as cast and melt-crystallized specimens. Despite the presence of a two-phase microstructure, the PEO microdomains in the as cast specimen do not act as reinforcing network tiepoints because they did not undergo crystallization during the solvent casting process and remained uncrystallized on storage at room temperature. Indeed, DSC heating curves measured from 300 to 360 K (instead of from 220 K as done in the study described in section a) did not show any endotherm for the as cast specimen. Also, no reflection was observed on the wide-angle X-ray diffraction photographs of the as cast specimen. These observations clearly indicate that the microdomain formation proceeded through a liquid–liquid phase separation during the casting process. Once the dispersion of the swollen PEO microphase had been formed, further evaporation of the solvent up to complete drying led to supercooled PEO microdomains dispersed in the polyisoprene matrix.

The crystallization of the supercooled PEO microdomains did not change appreciably the domain morphology in the PEO–PI–PEO specimen. This is shown in Figure 7 where a small-angle X-ray scattering (SAXS) curve measured on the as cast specimen (curve a) is compared to those measured on a specimen crystallized by cooling from 360 to 230 K (curve b) and on the same specimen obtained in the supercooled state by cooling from 360 K to room temperature (curve c). From Figure 7 one can see that a strong reflection occurs at about the same angle (2θ = 3.6 mrad) for the three specimens. The main difference between the three SAXS curves depicted in Figure 7 is a stronger reflection for the crystalline specimen than for the supercooled specimens. This can be explained by considering that the electron density of the crystalline PEO microdomains is higher than that of the supercooled microdomains. A second but a considerably weaker and diffuse reflection is observed at an angle 2θ close to 6.7 mrad on the SAXS curve of the crystalline specimen (curve b in Figure 7). Though not apparent on curves a and c in Figure 7, a second reflection at about the same angle was observed visually on the SAXS photographs of the two other specimens. Both reflections, which appeared as circular lines on the SAXS photographs of the unstretched specimens, deformed into ellipses with minor axis parallel to the stretching direction on the SAXS photographs taken on the crystalline specimen stretched at $\epsilon = 0.5$. This latter observation, together with the fact that the second reflection also appeared on the SAXS photographs of the supercooled specimens, indicates that both the strong and the weak reflections observed at angles 2θ close to 3.6 and 6.7 mrad, respectively, resulted from interdomain interferences. Attempts to rationalize these two reflections in terms of a lattice of spherical PEO microdomains failed. In fact, none of the possible cubic arrangements or even the hexagonal compact arrangement could justify the observation of a second-order reflection near 2θ = 6.7 mrad. On the other hand, a model based on a two-dimensional lattice of hexagonally packed cylinders would predict second-, and third-order diffraction lines at angles 2θ close to 6.2 and 7.2 mrad, respectively, assuming the strong reflection at 2θ = 3.6 mrad to be the first-order diffraction line. These values, which are only 1 mrad apart, appear in fair agreement with the observation of the diffuse reflection at 6.7 mrad. Though on the basis of the two reflections observed it is not possible to give a definite interpretation concerning the PEO-microdomain morphology, the above calculations suggest the presence of cylindrical PEO microdomains. However, considering the fact that the stress–strain curve measured on the crystallized PEO–PI–PEO specimen (Figure 6c) does not show either yield at low extension or significant stress softening during the first extension cycle at $\epsilon = 2.5$, it can be concluded that the PEO cylinders are relatively short. On the basis of a lattice of hexagonally packed cylinders, the interdomain distance calculated from the first-order diffraction (2θ = 3.6 mrad) would be 49 nm. From this latter value and the PEO volume fraction, $\varphi_{PEO} = 0.12$, estimated for the supercooled sample, one would obtain the value R = 9.0 nm for the radius of the PEO cylinders in the supercooled specimen. Interestingly, this value is close to the value R = 9.1 nm one can calculate from Meier's theory on amorphous block polymers,[20] which predicts the relationship $R_c = 1.0\alpha_c(r_0^2)^{1/2}$ between the radius, R_c, of the cylinders and the unperturbed root-mean-square end-to-end distance, $(r_0^2)^{1/2}$, of the end block. The value R = 9.1 nm was obtained by assuming the linear expansion factor $\alpha_c = 1$ and using the unperturbed dimension–molecular weight relationship $(r_0^2)^{1/2} = 0.084M^{1/2}$ nm reported in the literature for PEO at T = 298 K.[21]

(d) Mechanical Properties of the NaSCN-Complexed Material. As already mentioned, the PEO–PI–PEO film specimens complexed with NaSCN were prepared from benzene–methanol solutions. The initial volume fraction of methanol in the solvent was about 0.17, and the polymer concentration, c, was about 1%. Under these conditions a gel formed at an early stage ($c < 2\%$) during the solvent evaporation process, suggesting that the microdomain formation proceeded directly through the crystallization of the complexed PEO end blocks and not through a liquid–liquid phase separation as observed for the uncomplexed block polymer. Figure 8a shows stress–strain curves measured at 298 K on the as cast NaSCN-complexed material. Similar measurements made on the same material but recrystallized by slow cooling after melting at 470 K for 15 min are shown on Figure 8b. In each case one can observe stress–strain curves characteristic of a thermoplastic elastomer. Comparison of Figures

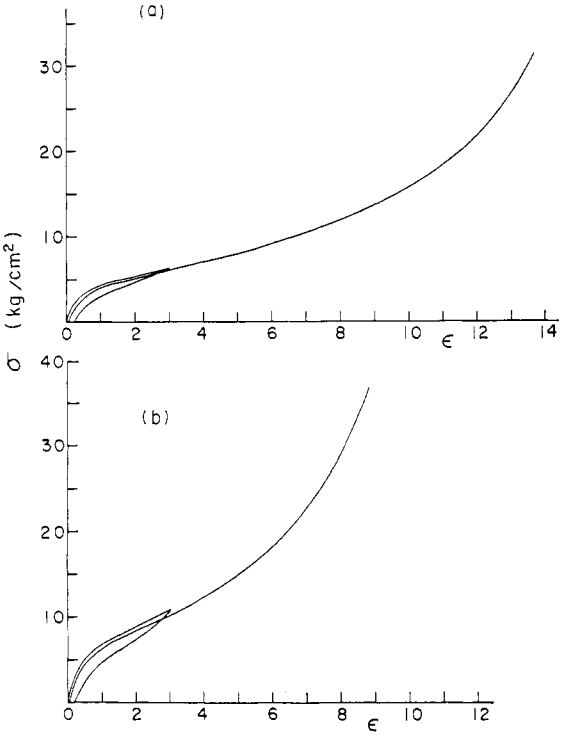

Figure 8. Stress–strain curves measured at 298 K on the PEO–PI–PEO block polymer complexed with NaSCN: (a) as cast from benzene–methanol solution, (b) recrystallized by slow cooling from 470 K to room temperature.

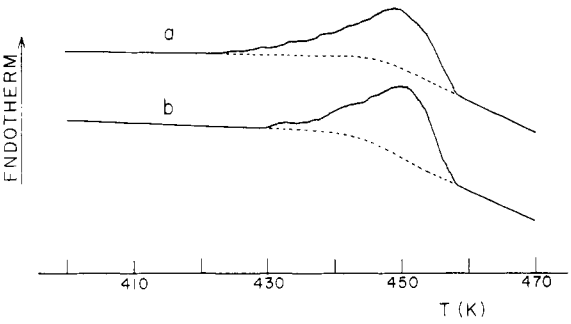

Figure 9. DSC heating curves measured at 10 K/min on the PEO–PI–PEO block polymer complexed with NaSCN: (a) as cast from benzene–methanol solution, (b) recrystallized by slow cooling from 470 K to room temperature.

8a and 8b shows that melt recrystallization results in an increase in tensile strength. For instance, the nominal tensile stresses, σ ($\epsilon = 2$), measured on the first extension curves at a strain $\epsilon = 2$ are 5.4 and 8.9 kg/cm^2 for the as cast and the melt-recrystallized specimens, respectively. Both values are lower than the corresponding value fo 13.7 kg/cm^2 measured on the crystallized uncomplexed specimen (Figure 6c), indicating a less effective network structure in the complexed materials. The nearly two-fold increase in σ ($\epsilon = 2$) produced by melt recrystallization of the complexed material is not associated with a significant increase in crystallinity. This is shown in Figure 9, where DSC heating curves measured before and after melt recrystallization of the complexed block polymer exhibit very similar melting endotherms. Although a slightly narrower melting peak is observed for the recrystallized material, the area under this latter peak is only a few percent greater than that of the as cast material.

Figure 10 shows SAXS curves measured before and after melt recrystallization of the complexed material. Either curve in Figure 10 exhibits a single reflection. This reflection occurs at an angle 2θ close to 5.4 mrad (Bragg spacing of 28 nm) for the as cast specimen, while it occurs at an angle close to 4.3 mrad (Bragg spacing of 36 nm) for the melt-recrystallized specimen. On the other hand, in either case the reflection, which appeared as a circular line on the SAXS photograph of the unstretched specimen, deformed into an ellipse on the SAXS photograph of the same specimen stretched at $\epsilon = 0.5$. Both these observations suggest that the change in mechanical properties produced by melt recrystallization is associated with an increase in interdomain distance resulting from a change in either microdomain size or microdomain morphology. Such a change can be rationalized by considering that the microdomain formation occurred in dilute solution ($c <$ 2%) through the crystallization of the complexed PEO chains. This would lead to a relatively large number of discrete microdomains that would remain isolated up to complete drying of the material. Because of their large number, these discrete microdomains should be close together and, upon melting at 470 K, merge into larger microdomains. This would explain the increase in Bragg spacing from 28 to 36 nm when measured before and after melt recrystallization of the complexed material. The formation of larger microdomains having greater internal cohesion and better capability to act as effective crosslinking entities would also explain the increase of tensile strength produced by melt recrystallization.

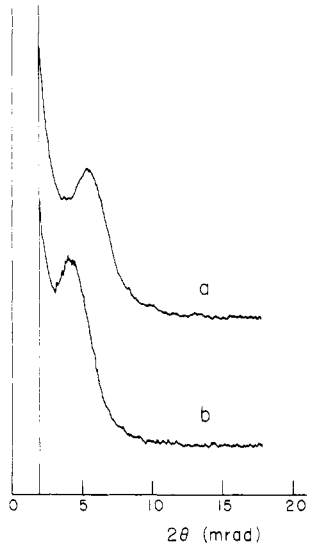

Figure 10. Small-angle X-ray scattering curves measured on the PEO–PI–PEO block polymer complexed with NaSCN: (a) as cast from benzene–methanol solution, (b) recrystallized by slow cooling from 470 K to room temperature.

Both the as cast and melt-recrystallized PEO–PI–PEO film specimens complexed with NaSCN retain their elastomeric behavior at temperatures well above room temperature. This is illustrated in Figure 11, which shows stress–strain curves measured at 373 K on the as cast material. Depicted in Figure 11 are two consecutive extension cycles recorded to a strain $\epsilon = 2$, followed by a third extension recorded up to rupture. As before, the specimen was relaxed for 15 min between each extension. Comparison of the mechanical behavior of the as cast complexed material measured at 373 K (Figure 11) with that of the same material measured at 298 K (Figure 8a) reveals a substantial decrease in tensile strength with increasing temperature. In fact, the nominal tensile stress, σ ($\epsilon = 2$), measured on the first extension curve at 373 K is about half that measured at 298 K. Nevertheless, the stress–strain data of Figure 11 show elastomeric nearly reversible extension cycles with a set after 15 min of relaxation that does not exceed the value of 10% observed at 298 K

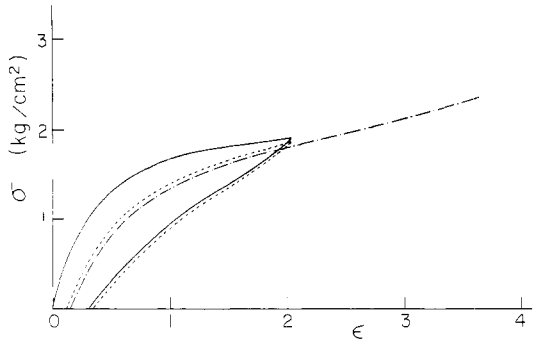

Figure 11. Stress–strain curves measured at 373 K for the as cast PEO–PI–PEO block polymer complexed with NaSCN. Represented are a first extension cycle (—), a second extension cycle (- - -), and a third extension (-·-) up to rupture.

(Figure 8a), indicating that the semicrystalline microdomains still act as reinforcing network tiepoints at 373 K. Note that at this latter temperature the PI matrix is 100 K above its glass transition temperature, so that the dimensional stability of the material observed during the extension cycles to a strain $\epsilon = 2$ cannot be due to the viscoelasticity of the PI matrix as it was in the preceding section for the supercooled uncomplexed block polymer. The twofold decrease in strength with increasing temperature from 298 to 373 K is significant if one considers that, according to the DSC curve of the present system (Figure 4), melting of the complexed PEO microdomains would start in the vicinity of 423 K. This loss of strength of the complexed material with increasing temperature must be attributed to the softening of the semicrystalline microdomains at temperatures well below their melting temperature. Such behavior is not a characteristic of the present system only. It has been observed for other ABA block polymers having crystalline end blocks, such as PES–PI–PES[1] (PES = poly(ethylene sulfide)) and polybutadiene-hydrogenated PB–PI–PB.[7] The reason for this behavior might be either softening of the amorphous component in the semicrystalline microdomains, or some premelting of the latter that could not be detected on the DSC curves, or both. In either case, the marked decrease of strength at temperatures well below the apparent melting temperature would be associated with deformation (at low strain) and disruption (at high strain) of the softened semicrystalline microdomains. At low strain, elastic deformation of the amorphous phase into the semicrystalline microdomains would account for the nearly reversible extension cycles observed on Figure 11.

Conclusion

In this study, it has been shown that a PEO–PI–PEO block polymer having a PEO weight fraction of 0.14 can be complexed with NaSCN to yield a semicrystalline thermoplastic elastomer that melts at about 450 K. Complexation occurs selectively with the PEO end blocks and does not affect significantly the thermal properties of the PI matrix. Contrary to the behavior of the uncomplexed material for which there are direct indications that liquid–liquid phase separation occurred during casting from benzene solution, it is thought that the complexed block polymer underwent crystallization at low concentration during casting from benzene–methanol solution. Some indications of this latter behavior are the formation of a gel at low concentration and the fact that melt recrystallization is necessary to achieve maximum mechanical properties of the complexed material. It has been shown that melt recrystallization of the complexed material increases the size of the semicrystalline microdomains but does not increase significantly their degree of crystallinity. Both the as cast and melt-recrystallized complexed materials exhibit good dimensional stability at high temperature. However, their strength appears to be considerably reduced with increasing temperature. This latter behavior seems to be a general characteristic of ABA elastomeric block polymers having semicrystalline end blocks. Another general characteristic of this class of block polymers is a pronounced supercooling of the crystallizable component when it is finely dispersed in the amorphous component. For instance, the present systems exhibit crystallization temperatures 60–90 K lower than those of the corresponding homopolymers. After Lotz and Kovacs,[15] it is proposed that this phenomenon occurs because the heterogeneous nuclei are segregated in a few isolated crystallizable microdomains and thereby cannot contribute to the nucleation of the greater part of the crystallizable component. In turn, it is proposed that the observation of a single stage of crystallization at a temperature well below that of the corresponding homopolymer is a clear indication that the semicrystalline component in block or graft polymers is finely dispersed into isolated microdomains.

Acknowledgment. This work was supported by the Natural Sciences and Engineering Research Council of Canada and the Quebec Ministry of Education.

References and Notes

(1) Hale, P. T.; Pope, G. A. *Eur. Polym. J.* **1975**, *11*, 677.
(2) Kuo, C.; McIntyre, D. *J. Polym. Sci., Polym. Phys. Ed.* **1975**, *13*, 1543.
(3) Hirata, E.; Ijitsu, T.; Soen, T.; Hashimoto, T.; Kawai, H. *Polymer* **1975**, *16*, 249.
(4) Foss, R. P.; Jacobson, H. W.; Cripps, H. N.; Sharkey, W. H. *Macromolecules* **1979**, *12*, 1210.
(5) Falk, J. C.; Schlott, R. J. *Macromolecules* **1971**, *4*, 152.
(6) Mohajer, Y.; Wilkes, G. L.; Wang, I. C.; McGrath, J. E. *Polym. Prepr., Am. Chem. Soc., Div. Polym. Chem.* **1980**, *21* (2), 191.
(7) Morton, M.; Lee, N. C.; Terrill, E. R. *Polym. Prepr., Am. Chem. Soc., Div. Polym. Chem.* **1981**, *22* (2), 136.
(8) Wright, P. V. *Br. Polym. J.* **1975**, *7*, 319.
(9) Parker, J. M.; Wright, P. V.; Lee, C. C. *Polymer* **1981**, *22*, 1305.
(10) Papke, B. L.; Ratner, M. A.; Shriver, D. F. *J. Phys. Chem. Solids* **1981**, *42*, 493.
(11) Pham, Q.-T.; Petiaud, R. "*Spectres RMN des Polymères* ^1H-^{13}C"; Editions SCM: Paris, 1980; Vol. 1, p 110.
(12) Wunderlich, B. "*Macromolecular Physics*"; Academic Press: New York, 1980; Vol. 3, p 67.
(13) O'Malley, J. J.; Crystal, R. G.; Erhardt, P. F. *Polym. Prepr., Am. Chem. Soc., Div. Polym. Chem.* **1969**, *10* (2), 796.
(14) Seow, P. K.; Gallot, Y.; Skoulios, A. *Makromol. Chem.* **1976**, *177*, 177.
(15) Lotz, B.; Kovacs, A. J. *Polym. Prepr., Am. Chem. Soc., Div. Polym. Chem.* **1969**, *10* (2), 820.
(16) O'Malley, J. J. *J. Polym. Sci., Part C* **1977**, *60*, 151.
(17) Turnbull, D. *J. Appl. Phys.* **1949**, *20*, 817.
(18) Cormia, R. L.; Price, F. P.; Turnbull, D. *J. Chem. Phys.* **1962**, *37*, 1333.
(19) Koutsky, J. A.; Walton, A. G.; Baer, E. *J. Appl. Phys.* **1967**, *38*, 1832.
(20) Meier, D. J. In "Block and Graft Copolymers"; Burke, J. J., Weiss, W., Eds.; Syracuse University Press: Syracuse, NY, 1973; p 105.
(21) Beech, D. R.; Booth, C. *J. Polym. Sci., Polym. Phys. Ed.* **1969**, *7*, 575.